# Effect of passive structure on MHD stability in the EAST tokamak

G. J. Liu,[1, a)] B. N. Wan,[1] Y. W. Sun,[1] Y. Q. Liu,[2] and W. F. Guo[1]
[1)] *Institute of Plasma Physics, Chinese Academy of Sciences, PO Box 1126, Hefei 230031, People's Republic of China*
[2)] *Euratom/UKAEA Fusion Association, Culham Science Centre, Abingdon, OX14 3DB, United Kingdom*

## I. INTRODUCTION

One of the most important missions of Experimental Advanced Superconducting Tokamak (EAST) is to demonstrate high performance and steady state operation in ITER-like plasma configuration with superconducting equilibrium field coils. Advanced tokamak concepts require high beta, which will exceed "Troyon beta limit" and lead to resistive wall mode (RWM). The elongated plasmas are inherently unstable against vertical displacement. Therefore, it is necessary to increase the plasma beta limit determined by RWM and control of vertical instability. The passive plate can increase both of these two stability limits. The effect of passive plate on vertical instability and resistive wall mode (RWM) (simulate by MARS) in the EAST tokamak is presented.

The effect of passive plates on vertical displacement control in EAST tokamak is investigated by open loop experiments and numerical simulations based on a rigid displacement plasma model. The instability growth rates and the stability margin are gain by using the Eigen mode analysis. The experiments and simulations indicate that the vertical instability growth rates are is reduced by a factor of about 2 in the presence of the passive plates, where the adjacent segments are not connected to each other. The operational window is greatly enlarged with the passive plates.

The effect of the passive plate on the external kink and RWM on EAST will be modeled by using the MARS code. The effect of plasma shape, pressure and current density profiles, the rotation velocity and profiles on the stability boundary of the external kink and RWM on EAST are still on-going and will be discussed in detail.

## II. PASSIVE STRUCTURE ON EAST

EAST is designed to be up-down symmetric, as shown in Figure 1. It is equipped with a set of 12 superconducting PF coils around the vacuum vessel and a pair of water-cooled copper coils inside the vacuum vessel (IC).

Passive structure on EAST contains vacuum vessel made of 8mm thick stailess steel plates and passive plate plates made of 16 copper alloy segments with 30mm in thick and 350mm in width.

[a)] gjliu@ipp.ac.cn

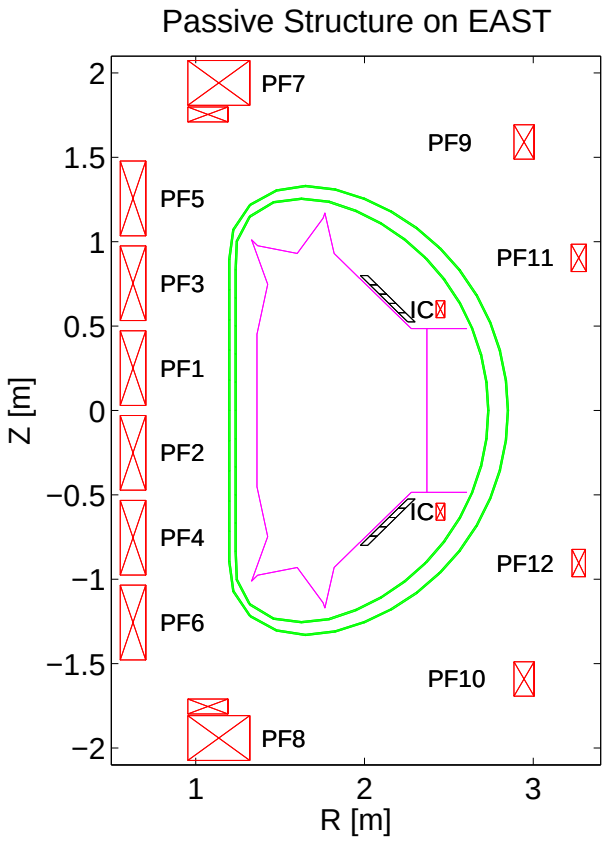


FIG. 1. *Arrangement of the 12 PF coils (PF 1-12), active feedback coils (IC), vacuum vessel(green lines) and the passive plate loops (black lines) on the poloidal cross section of EAST.*

## III. THE EFFECT OF PASSIVE PLATE ON VDE

### A. Theoretical model

The rigid displacement model is employed in the simulation. It is assumed in this model that, the plasma current shifts rigidly with neither re-distribution nor surface currents during the vertical displacement of the plasma column. Further assumptions are also made: negligible inertia, axisymmetric displacements, negligible horizontal-direction displacement and constant total plasma current. In tokamak plasma experiments, these assumptions are valid in the case of small displacement.

The model can be described by the following circuit equation:[12]

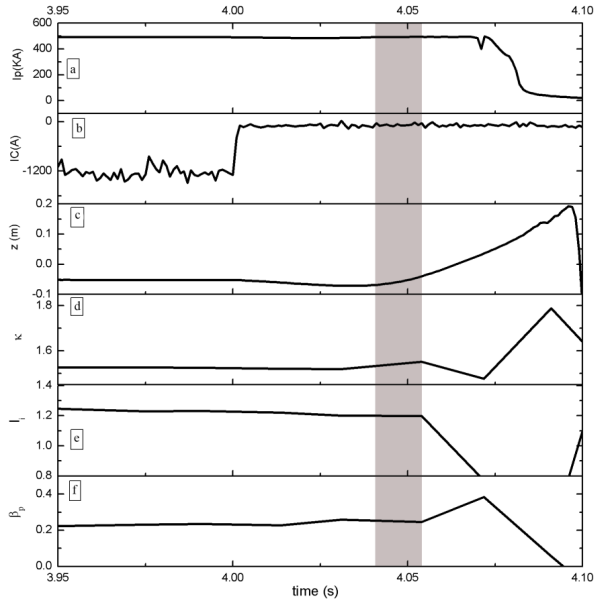


FIG. 2. *The time evolution of plasma current (a), active feedback current (b), plasma central position (c), elongation $\kappa$ (d), internal inductance $l_i$ (e) , and poloidal plasma beta $\beta_p$ (f) in shot 36795 on EAST.*

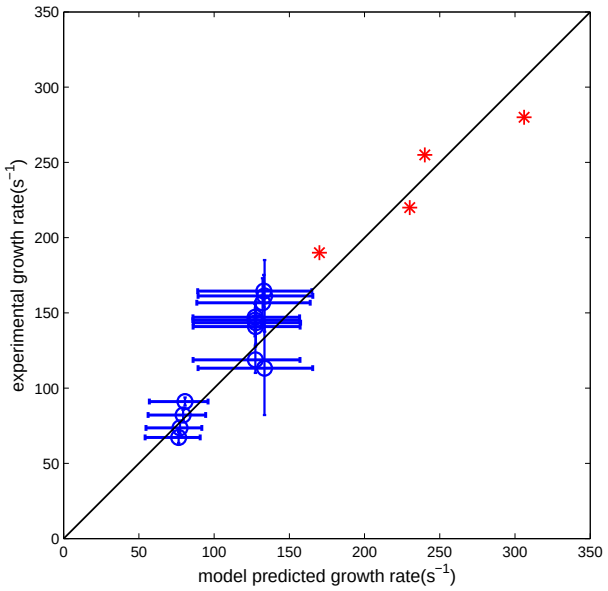


FIG. 3. *Observed growth rate versus model predicted growth rate. The open circle represent the results with the passive plate resistance being $2m\Omega$ , where the horizontal error bars denote uncertainties in resistance, and vertical error bars refer to experimental fitting errors. The star points represent the results without passive plates*

$$L_{ss}\dot{I}_s + R_{ss}I_s + \frac{\partial \psi_{sp}}{\partial z}\dot{z} = V_s \tag{1}$$

where $L_{ss}$ is the mutual inductance matrix between mesh currents of the passive structure and PF coils, $R_{ss}$ is the resistance matrix of the conductor structure, $I_s$ and $V_s$ are vectors of current and voltage of the conductor structure respectively, $\psi_{sp}$ is the flux at the conductor structure due to plasma current profile, $\dot{x}$ is the time derivative of $x$, and the subscript $s$ and $p$ refer to the passive structure and the plasma.

The growth rate of vertical instability can be written as,

$$\gamma = max\{eig\left(-R_{ss}^{-1}L_{ss}^{*}\right)\} \tag{2}$$

The stability margin is defined as:

$$m_s = max\{eig\left(-L_{ss}^{-1}L_{ss}^{*}\right)\} \tag{3}$$

where:

$$L_{ss}^{*} = L_{ss} - \frac{\partial \psi_{sp}}{\partial z}\frac{\partial z}{\partial I_s} \tag{4}$$

### B. Open loop experiments and numerical simulations

The open loop experiments are carried out with and without passive plate to detect the growth rate of vertical instability. As shown in Figure 2, the proportional-integral-differential (PID) feedback gains for vertical position are set to be zero at 4 s; thereafter the IC current is switched off (Figure 2 (b)) and plasma control system releases the control for vertical position. The plasma vertical position drifts exponentially from its initial equilibrium position starting at about 4.03s as shown in Figure 2 (c).

The comparison between the observed growth rates and the predicted ones is shown in Figure3. The model predicted vertical instability growth rates accord well with the observed ones within the uncertainties in the resistance of the passive plate.

Compared with the results without the passive plate, the vertical instability growth rates with passive plate are reduced by a factor of about 2, although the plasma parameters are similar in these two cases.

The used equilibrium configurations are generated from EFIT code based on EAST designed parameters. The plasma current and triangularity are fixed at $I_p = 1MA, \delta = 0.5$, and other effective parameters $\beta_p, \kappa, l_i$ are scanned. The stability margin and vertical growth rate are evaluated from Eqs.2 and 3. The simulation results are presented in Figures 4,5 and 6.

## IV. PRELIMINARY STUDY OF RESISTIVE WALL MODE RESEARCH ON EAST

### A. basic equations in MARS

There are no RWM has been observed on EAST, but some preliminary study has developed by numerical sim-

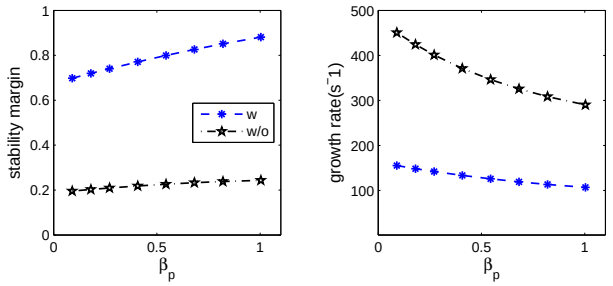


FIG. 4. *Dependences of the stability margin (top) and vertical instability growth rate (bottom) on* $\beta_p$ *with* $\kappa = 1.93 \pm 0.02, li = 0.945 \pm 0.04, A = 3.95 \pm 0.02$.

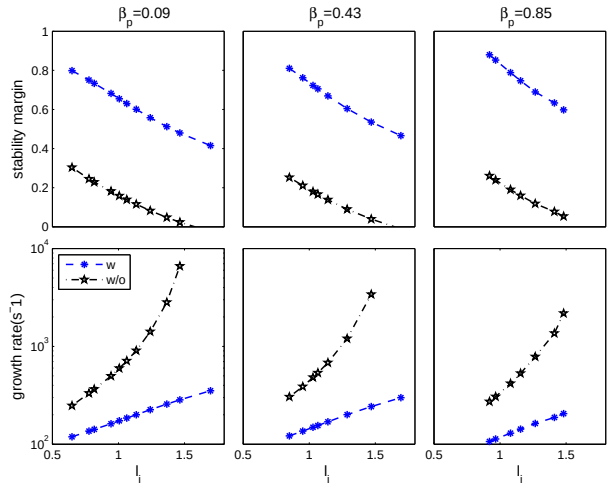


FIG. 5. *Dependences of stability margin (top) and vertical instability growth rate (bottom) on li with* $\kappa = 1.93 \pm 0.02, A = 3.95 \pm 0.02, \beta_p = 0.09(left), \beta_p = 0.43(middle), \beta_p = 0.85(right)$.

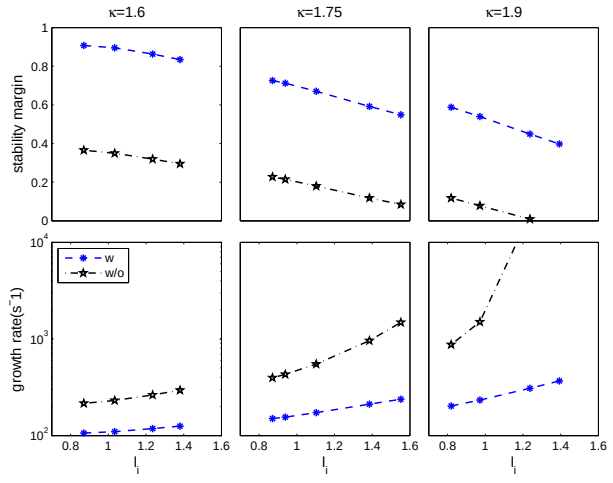


FIG. 6. *Dependences of stability margin (top) and vertical instability growth rate (bottom) on li with* $\beta_p = 0.43 \pm 0.02, A = 3.95 \pm 0.02, \kappa_p = 1.6(left), \kappa = 1.75(middle), \kappa = 1.9(right)$.

ulation by MARS.[34567]

MARS is a linear plasma stability code which was first constructed by Bondeson et al. and developed by Y. Q. Liu et al. for the study of nonideal plasma instabilities. It is an eigenvalue code with the complex growth rate being the eigenvalue. In this code is that the growth rate enters the equation directly and not its square as is usually the case for other ideal MHD stability codes. Therefore, MARS is particularly suited for the study of unstable modes with very low growth rates as is the case of resistive MHD modes and the RWMs.

The basic equations in MARS are:

$$(\gamma + in\Omega)\,\vec{\xi} = \vec{v} + \left(\vec{\xi}\cdot\nabla\Omega\right) R^2\nabla\phi \tag{5}$$

$$\begin{aligned}\rho\,(\gamma + in\Omega)\,\vec{v} = &-\nabla\cdot\overleftrightarrow{p} + \vec{j}\times\vec{B} + \vec{J}\times\vec{b}\\ &-\rho\left[2\Omega\hat{Z}\times\vec{v} + (\vec{v}\cdot\nabla\Omega)\,R^2\nabla\phi\right]\\ &+\nabla\cdot\left(\rho\vec{\xi}\right)\Omega\hat{Z}\times\vec{V}_0\\ &+\rho\kappa_{\|}\left|k_{\|}\right| v_{th,i}\left[\vec{v}\cdot\hat{b} + \left(\vec{\xi}\cdot\nabla\right)\vec{V}_0\cdot\hat{b}\right]\hat{b}\end{aligned} \tag{6}$$

$$\rho\,(\gamma + in\Omega)\,\vec{b} = \nabla\times\left(\vec{v}\times\vec{B}\right) + \left(\vec{b}\cdot\nabla\Omega\right) R^2\nabla\phi - \nabla\times\left(\eta\vec{j}\right) \tag{7}$$

$$\vec{j} = \nabla\times\vec{b} \tag{8}$$

$$\rho\,(\gamma + in\Omega)\,p = -\vec{v}\cdot\nabla P - \Gamma P\nabla\cdot\vec{v} \tag{9}$$

$$p_{\|} = p_{\|}^{kinetic} \tag{10}$$

$$p_{\perp} = p_{\perp}^{kinetic} \tag{11}$$

### B. Troyon $\beta_N$ limit on EAST

An equilibrium from 38300@3000ms on EAST is used for troyon $\beta_N$ limit research. The major paraments are: $R_0 = 1.75m$, $B_0 = 1.832T$, $I_p = 400kA$, $q_0 = 1.36$, $q^* = 7.5$, $a/R = 4.23$.

To research the effect of passive structure on $\beta_N$ limit, the passive plate is expanded to a close surface. And in this close surface, the conductivities of the grids in the passive plate are assigned according to the estimated resistance of passive plate ($2m\Omega$), while the conductivities of the other grids are zero.

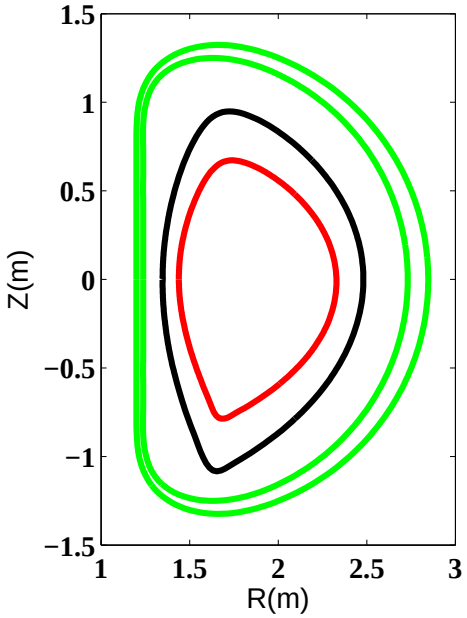


FIG. 7. *Equilibrium,38300@3000ms on EAST. The green, black and red lines stand for vacuum vessel, passive plate surface and last close magnetic surface, separately*

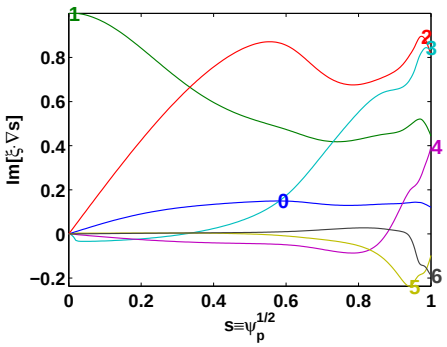


FIG. 8. *Perturbation displacement VS $\psi_p$ when RWM is unstable*

The two vacuum vessels, passive plate surface, and last close magnetic surface are divided into 301 grids separately. The equilibrium is shown in Figure 7.

The $\beta_N$ is scanned by fixing total plasma current and current profile and changing the plasma pressure. And when RWM is unstable, one example of the perturbation displacement is shown in Figure 8

The calculated of $\beta_N$ limit of no wall and ideal wall are shown in Figure 9

### C. Future work of RWM on EAST

In the future, the effect of plasma shape, pressure and current density profiles, the rotation velocity and profiles and on the stability boundary of the external kink and

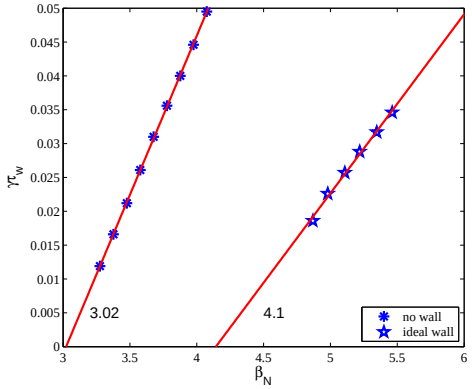


FIG. 9. *beta$_n$ limit of no wall and ideal wall in equilibrium, 38300@3000ms, EAST*

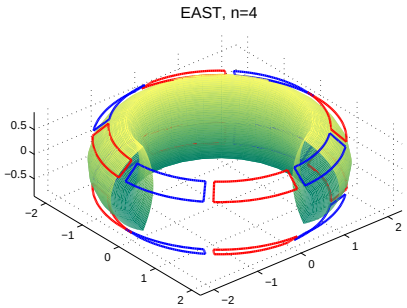


FIG. 10. *RMp coils on EAST*

RWM and the control of RWM by RMP coils will be studied by numerical simulation and tokamak experiments on EAST.

## V. REFERENCES

[1] A. Portone, Nuclear fusion **45**, 926 (2005).
[2] G. J. Liu, B. N. Wan, J. P. Qian, Y. W. Sun, B. J. Xiao, B. Shen, Z. P. Luo, X. Ji, and S. L. Chen, Chinese Physics B **21**, 085201 (2012).
[3] A. Bondeson, Y. Liu, D. Gregoratto, Y. Gribov, and V. Pustovitov, Nuclear fusion **42**, 768 (2002).
[4] A. Bondeson and D. Ward, Phys Rev Lett **72**, 2709 (1994).
[5] Y. Liu, M. Chu, I. Chapman, and T. Hender, Physics of plasmas **15**, 112503 (2008).
[6] H. Ltjens, A. Bondeson, and O. Sauter, Computer physics communications **97**, 219 (1996).
[7] M. Chu and M. Okabayashi, Plasma physics and controlled fusion **52**, 123001 (2010).